Decoupled Speed and Torque Control of IPMSM Drives Using a Novel Load Torque Estimator

Mohamed ZAKY[1,2*], Ehab ELATTAR[2], Mohamed METWALY[2]
[1]*Department of Electrical Engineering, Northern Border University, Arar,1321, Saudi Arabia*
[2]*Department of Electrical Engineering, Minoufiya University, Shebin El-Kom, 32511, Egypt*
[*]*mszaky78@yahoo.com*

***Abstract*—This paper proposes decoupled speed and torque control of interior permanent magnet synchronous motor (IPMSM) drives using a novel load torque estimator (LTE). The proposed LTE is applied for computing a load torque and yielding a feed-forward value in the speed controller to separate the torque control from the speed control. Indirect flux weakening using direct current component is obtained for high speed operation of the IPMSM drive, and its value for maximum torque per ampere (MTPA) control in constant torque region is also used. LTE uses values of direct and quadrature currents to improve the behavior of the speed controller under the reference tracking and torque disturbances. The complete IPMSM drive by Matlab/Simulink is built. The effectiveness of the proposed control scheme using an experimental setup of the complete drive system implemented on a DSP-DS1102 control board is confirmed. Extensive results over a wide speed range are verified. The efficacy of the proposed method is confirmed in comparison to a conventional PI controller under both the reference speed tracking and load torque disturbance.**

***Index Terms*—proportional integral controller, load torque estimator, speed control, flux weakening region, maximum torque per ampere, interior permanent magnet synchronous motor.**

I. INTRODUCTION

Vector control theory has considerably improved the performance of AC drives as separately excited dc motors. Interior permanent-magnet synchronous motors (IPMSMs) are considered as an important machine that used in industrial applications [1-2]. They have several advantages such as low expensive, high efficiency, high torque to current ratio, high power-to-weight ratio, etc. The ability of IPMSM to work in a flux-weakening (FWR) region is considered an advantage. This allows for operating above the rated speed at constant voltage. This enables for minimizing the harmonic losses of the IPMSM [3-6]. However, their operation over a wide speed range in both constant torque region (CTR) and constant power region (CPR) is still a challenge. The complexity arises due to the coupling influence between the speed and currents. Moreover, the magnetic saturation of the rotor core causes a nonlinearity of the developed torque [7-9].

Several control methods for IPMSM were presented in [10-19]. High speed operation above a nominal speed can be developed using flux weakening (FW) algorithms. A direct flux weakening of the IPMSM is not allowable directly. Therefore, indirect flux weakening using i_d is used as a function of the speed and quadrature axis current i_q by minimizing the air gap flux using its demagnetizing effect [10]. Thus, traditional control methods using $i_d = 0$ are incapable of driving the IPMSM drive at high-speeds with guaranteeing the nominal limits of the current, the voltage, and the power. It is well-known that the motor voltage value exceeds with increasing the motor speed or i_q using $i_d = 0$. Consequently, instability of the IPMSM drive may be occurred due to the saturation of the current regulators at high speeds at a certain torque [11]. Control of IPMSM drive with assuming that $i_d = 0$ for simplification prevents to employ the reluctance torque of the IPMSM. So, erroneous results at different conditions are occurred. Moreover, the desired performance cannot be maintained. Fuzzy logic controller (FLC)-based speed control in the maximum torque per ampere (MTPA) for IPMSM drive was proposed [12]. A linear torque control method has been presented in [13] to simplify the controller and employ the reluctance torque. In [14], adaptive self-tuning MTPA has been presented. High-speed operation of IPMSM by modified FLC with genetic approach was offered in [15]. To develop the behavior for IPMSM in FW region, the machine parameters were estimated in [16]. To ensure a large efficiency, FLC with minimizing the losses was presented in [17]. Two distinct FLCs has been proposed in [18] by adapting the PWM hysteresis band and the other FLC uses a tuned PI controller. To get accurate torque for IPMSM drives, the reluctance torque was estimated and employed in MTPA [19]. Optimization of the efficiency of IPMSM drives was presented in [20] using two fuzzy controllers. MTPA and FW controls were introduced in [21] with estimation of the parameters. A speed controller using a wavelet-neural-network of IPMSM drives was designed using the speed error and its change [22]. A robust nonlinear speed controller for IPMSMs based on MTPA with harmonic decrease was accomplished in [23]. Linear FW torque and current control of IPMSM was presented in [24].

The precise speed control has been needed for high-performance IPMSM drives [25]. The speed controller should have a rapid response, strong to disturbances and parameters variation. To ensure these control issues, proportional–integral (PI) schemes were employed in DC and AC motor drives due to their simplicity [26]. But, they are inappropriate for high dynamic performance drives. Since they are sensitive to parameters changes and torque fluctuations [27]. This affects decoupling characteristics for field oriented control. To improve the performance of the PI controllers, their gains should be adapted to give the desired performance under speed tracking trajectory, machine

The authors wish to acknowledge the approval and the support of this research study by the grant no. ENG-2016-1-6-F-4670 from the Deanship of Scientific Research in Northern Border University, Arar, KSA.

Digital Object Identifier 10.4316/AECE.2017.03003

parameters variation and load torque changes [28-29]. A speed controller insensitive to machine parameters and load torque changes for a PMSM was designed in [30]. To overcome difficulties using PI scheme, load torque estimator (LTE) is used in conjunction with the PI controller. LTE is an effective method that improves the system performance without extra sensors or changing the input-output hardware of the system [31-33].

The previous works, which presented in [31-33] using LTE, were restricted to conditions without considering FW into account. Moreover, the previous LTE depends only on i_q with $i_d = 0$. Therefore, there exists a need to extend LTE to the FW mode of operation. So, the main contribution is to apply and implement the proposed control algorithm in the FW region. Also, an integrated nonlinear equation of LTE using i_d and i_q is designed for MTPA, FW, and LTE operation.

The major aims are to improve dynamic behavior for IPMSM drives using a PI controller in conjunction with LTE for MTPA and FW regions. This method estimates the load torque to add a load torque component in the reference i_q^*. As a consequence, the electromagnetic torque is divided into two components. A feed-forward component recovers the load torque changes, and the dynamic component adapts the speed variation. The proposed novel LTE depends mainly on i_q and i_d, and differs from the previous works that use i_q only. To validate the efficacy of the proposed approach, a simulation model of the IPMSM drive can be assembled using Matlab/Simulink. The simulation results show the high dynamic behavior of the PI controller with LTE in comparison to the conventional PI controller under speed tracking and load torque changes. An experimental setup of the complete drive system is implemented on a DSP-DS1102 platform to justify the effectiveness of the proposed method.

II. IPMSM Model

A. Dynamic Model

An IPMSM mathematical model is described as given in [10]:

$$\begin{bmatrix} V_q \\ V_d \end{bmatrix} = \begin{bmatrix} R_s + pL_q & \omega_r L_d \\ -\omega_r L_q & R_s + pL_d \end{bmatrix} \begin{bmatrix} i_q \\ i_d \end{bmatrix} + \begin{bmatrix} \omega_r \lambda_m \\ 0 \end{bmatrix} \quad (1)$$

$$T_e = \frac{3}{2} P \left[\lambda_m i_q + \left(L_d - L_q \right) i_d i_q \right] \quad (2)$$

$$T_e = \frac{J}{P} \dot{\omega}_r + \frac{B}{P} \omega_r + T_L \quad (3)$$

where, V_d, V_q are d-q stator voltages, i_d, i_q are d-q stator currents, R_s is stator resistance, L_d, L_q are d-q stator inductances, T_e, T_L are motor and load torques, J is moment of inertia, B is friction coefficient, P is number of pair poles, p *is* differential operator, λ_m is rotor magnetic flux linkage, and ω_r is speed.

B. Torque-Speed Characteristics of IPMSM

Fig. 1 illustrates the torque-speed characteristics of the IPMSM during the complete operating range. This range is divided into two regions. The CTR is under a nominal speed with maintaining a constant flux. The direct current is set $i_d \neq 0$ to ensure a MTPA. The other region is a CPR beyond a nominal speed with variable flux which is called the FW region.

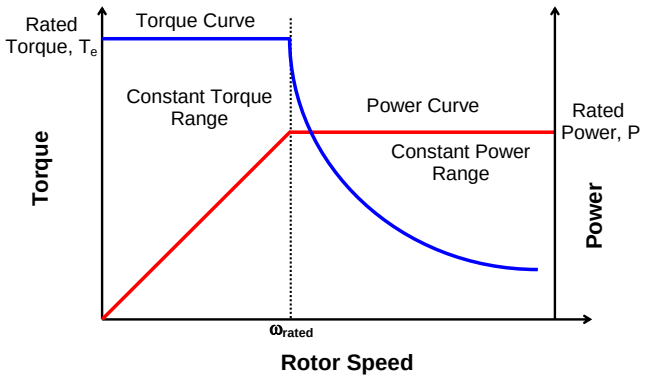

Figure 1. Torque-speed characteristics during constant torque and constant power regions

C. Control Problem Statement

The developed torque using (3) depends mainly on two terms $\lambda_m i_q$ and $(L_d - L_q) i_d i_q$. The first term describes a torque component owing to a rotor PM flux. The second term describes a reluctance torque component owing to product of $(L_d - L_q)$ and $i_d i_q$. In conventional control methods of IPMSM during the CTR, id is assumed to be zero. Then, the control of IPMSM is simplified and the equation of torque and quadrature current becomes linear. This achieves a linear torque control approach similar to a separately excited DC motors. Nevertheless, this means that the reluctance torque of the machine is not used. Therefore, an erroneous is occurred under this assumption because the maximum torque capability of the machine is not allowed under various operating conditions. Moreover, with id = 0, the d-axis flux linkage relies on the rotor PM alone. So, this control constraint is inappropriate to work in FW region under the rated capabilities of the inverter and the IPMSM.

In other methods of IPMSM, the control is managed with id ≠ 0. Therefore, the torque control is considered nonlinear and the reluctance torque is employed. Using the reluctance torque is very essential to enhance the operation in FW and improve the efficiency. Therefore, several approaches are presented using nonlinear torque control principle to employ the benefit of the reluctance torque and to accomplish the desired targets. In nonlinear torque control approaches, iq is developed based on the torque command. Then, id is calculated according to the value of iq and the speed reference to ensure the desired task. Therefore, control difficulty of IPMSM arises under nonlinear torque control feature if uncertainties and disturbances will occur.

Accurate speed trajectory tracking under changes of speed and torque commands or parameters deviations is a highly required objective. Therefore, traditional PI controllers are

unable to accomplish wanted behavior under these constraints. Thus, the most important contribution is to develop a modified PI with a LTE to manage these issues. A direct stator current id is designed to operate in both MTPA and FW, respectively. The integrated PI speed controller with LTE, MTPA, and FW approaches works well during a wide speed range. The LTE technique in conjunction with PI controller, which principally adjusts iq, provides a good tracking performance under uncertainties and disturbances. The IPMSM behavior is improved by designing the stator current id based on iq to maintain the current and voltage around a rated value of the inverter and motor. This provides a good behavior in comparison to conventional methods with id =0.

III. Control Algorithms of IPMSM

A. Control Algorithm of CTR

The control algorithm for CTR to obtain a MTPA can be derived as follows. The stator phase voltage can be described by (4) [10]:

$$V_a = v_d + jv_q \tag{4}$$

where, V_a is phase stator voltage.

The stator phase current can be expressed using (5).

$$I_a = i_d + ji_q \tag{5}$$

In CTR under rated speed, I_a is assumed to be constant at its maximum value. So, i_d can be deduced related to i_q for ensuring a MTPA control. The following procedure is followed.

The first derivative of (1) relating to i_q is derived. Then, the resultant equation is equating to zero for maximum value. This yields i_d^* for MTPA,

$$i_d^* = \frac{\lambda_m}{2(L_d - L_q)} - \sqrt{\frac{\lambda_m^2}{4(L_d - L_q)^2} + i_q^{*2}} \tag{6}$$

where, i_d^*, i_q^* are the reference d-q stator currents.

To reduce the calculation time for real-time implementation, a Taylor series expansion around $i_q^* = 0$ is applied to (6). The following equation can be developed as given in [10].

$$i_d^* = -\frac{(L_q - L_d)}{\lambda_m} i_q^{*2} = K_d i_q^{*2} \tag{7}$$

where, $K_d = \dfrac{(L_d - L_q)}{\lambda_m}$

B. Control Algorithm of Constant Power Region

In CPR beyond a rated speed, i_d^* is obtained relating to i_q^* for keeping V_a at its maximum value. Using (1), (2), and (3) with neglecting stator resistance voltage drop, i_d^* can be calculated as given in (8).

$$i_d^* = -\frac{\lambda_m}{L_d} + \frac{1}{L_d}\sqrt{\frac{(V_m')^2}{P^2\omega_r^2} - L_q^2 i_q^{*2}} \tag{8}$$

where, V_m' is maximum stator voltage without resistance voltage drop.

The relation between i_d^* and i_q^* from (8) is drawn as shown in Fig. 2. The trajectory describes an ellipse in the *d-q* axis plane. It is found that if the speed rises in the FW region, the change of current vector is very small. To reduce the calculation burden, (8) can be simplified as given in (9), [10]. It represents a very important equation to control above the rated speed of 157 rad/sec.

$$i_d^* = -\frac{1}{L_d}\left(\lambda_m - \frac{V_m'}{P\omega_r} + \frac{L_q^2 i_q^{*2} P\omega_r}{2V_m'}\right) \tag{9}$$

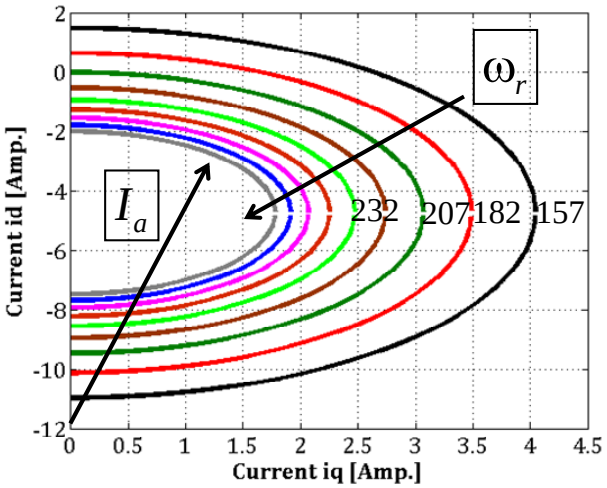

Figure 2. Locus trajectory between iq and id at different speeds starting from 157 to 357 rad/s in a step of 25 rad/s

C. Maximum Speed

To obtain the maximum speed ω_{rmax} , (10) can be derived from (8) with i_q^* = 0 to provide the maximum speed for a certain stator voltage and current.

$$\omega_{r\max} = \frac{V_m'}{P(L_d I_a + \psi\ )} = \frac{\sqrt{V_m^2 - (R_s I_a)^2}}{P(L_d I_a + \lambda_m)} \tag{10}$$

where, V_m is maximum stator voltage.

IV. Design of the Proposed Speed Control Algorithms

A. Load Torque Estimation

Load torque estimation is highly desired by adding a component to compensate the quadrature current component i_q. This improves the behavior of the speed controller, particularly under disturbances. However, the value of the load torque is required for the feed-forward compensation. If a torque transducer is employed for measuring the torque, this will add an extra cost. To overcome this obstacle, an estimation of the load torque is used in this paper.

Using (3) yields,

$$\frac{B}{P}\omega_r + \frac{J}{P}\frac{d\omega_r}{dt} = T_e - T_L \tag{11}$$

Then, (2) can be rewritten as follows,

$$T_e = K_{t1} i_q^* + K_{t2} i_d^* i_q^* \tag{12}$$

where,

$$K_{t1} = \left(3/2\right) P \lambda_m \tag{13}$$

$$K_{t2} = \left(3/2\right) P \left(L_d - L_q\right) \tag{14}$$

The purpose of the LTE is to give a feed-forward component in the speed controller. The goal is to separate the torque control from the speed control. Thus, the torque equation can be partitioned into two components. A feed-forward load torque component T_{eT_L} is to recover the load torque. The second component is the speed-dependant torque component $T_{e\Delta\omega}$ to recover the speed dynamic variation.

Therefore, (3) becomes

$$T_e = T_{eT_L} + T_{e\Delta\omega} = T_L + \frac{J}{P}\frac{d\omega_r}{dt} + \frac{B}{P}\omega_r \tag{15}$$

where,

$$T_{eT_L} = T_L \tag{16}$$

and

$$T_{e\Delta\omega} = \frac{J}{P}\frac{d\omega_r}{dt} + \frac{B}{P}\omega_r \tag{17}$$

The component $T_{e\Delta\omega}$ is provided by the speed controller to deal with the speed dynamics, and the component T_{eT_L} is given by the load torque estimation to compensate for torque disturbances. The motor torque cannot be directly recognized. Therefore, it can be calculated using i_q. Then, T_L can be calculated using a motor torque and a variation of the motor speed. (15) can be used to estimate T_L.

$$\begin{aligned}\hat{T}_L &= T_{eT_L} = T_e - T_{e\Delta\omega} \\ &= K_{t1} i_q^* + K_{t2} i_d^* i_q^* - \frac{J}{P}\frac{d\omega_r}{dt} - \frac{B}{P}\omega_r\end{aligned} \tag{18}$$

The principle of compensation of the speed controller is to adjust the reference input by a feed-forward term for enhancing the dynamic control behavior. This development is highly suitable for industrial systems because it is capable of improving the performance without adding a hardware sensor. Also, the system cost is not influenced.

The estimated load torque $\hat{T}_L$ improves the reference current i_q^* by giving the following component,

$$i_{qT_L} = \frac{\hat{T}_L}{K_{t1} + K_{t2} i_d^*} \tag{19}$$

This component is can be derived according to the operating region. In case of the CTR, i_d can be replaced by (7). Then, (19) can be rewritten for CTR as follows,

$$i_{qT_L} = \frac{\hat{T}_L}{K_{t1} + K_{t2} K_d i_q^{*2}} \tag{20}$$

Alternatively, (19) can be rewritten for CPR using (9) as follows,

$$i_{qT_L} = \frac{\hat{T}_L}{K_{t1} - \frac{K_{t2}}{L_d}\left(\lambda_m - \frac{V_m'}{P\omega_r} + \frac{L_q^2 i_q^{*2} P \omega_r}{2V_m'}\right)} \tag{21}$$

This is the novel contribution of the current paper in comparison to the previous works that calculate LTE from i_q only and ignoring the value of i_d. The speed controller provides a value for i_q^* to indirectly adjust the torque. The key object of the LTE is to add a component to i_q^* to improve the dynamic performance under disturbances. The total value of i_q^* can be designed as described in (22).

$$i_q^* = i_{qT_L} + i_{q\Delta\omega} \tag{22}$$

The structure of the proposed PI controller using a feed-forward LTE is demonstrated in Fig. 3. The construction of the whole IPMSM drive with proposed control approaches is demonstrated by Fig. 4.

The structure of the field oriented control of the IPMSM is demonstrated in Fig. 4. It consists of four major segments. They compose from the feedback speed controller, feedback current controller, the voltage source inverter with its gate drive circuit, and the IPMSM and its mechanical load. The reference speed is compared with the actual one and the error is adjusted by the speed controller. The output is considered the reference quadrature current component i_q^*. The reference direct current component i_d^* is calculated using (7) for CTR and (9) for CPR. These two currents in *dq*-axis are transformed to the three-phase reference currents which compared by the measured ones. The current errors are passed through the hysteresis current controller which yields gate pulses. Then, the voltage source inverter drives the IPMSM with three-phase voltages of controlled magnitude and frequency.

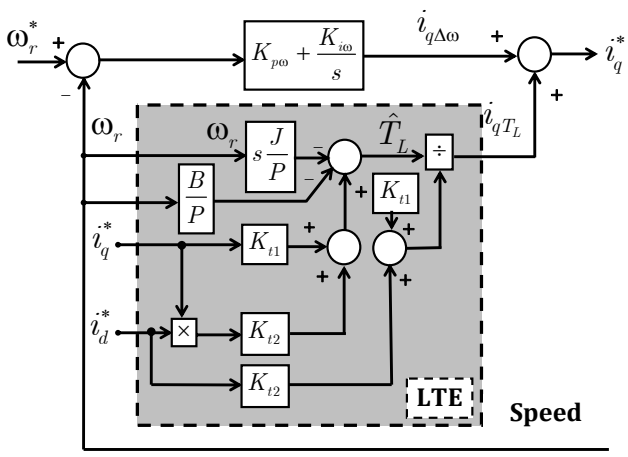

Figure 3. Schematic drawing of the PI controller with proposed LTE

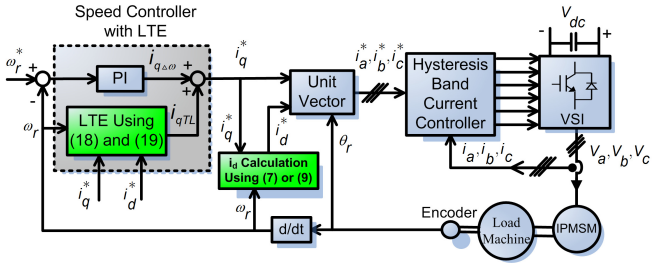

Figure 4. Schematic diagram of the field oriented control of the IPMSM below and above rated speed using the proposed LTE with MTPA or FW control algorithms

V. Simulation Results

The effectiveness of the proposed speed controller with LTE approach needs to be validated by simulation results.

The complete IPMSM drive with the proposed and traditional speed approaches is performed under MATLAB/Simulink. The schematic IPMSM drive system of Fig. 4 is employed. The LTE structure of Fig. 3 can be utilized in conjunction with the PI speed controller. The direct current i_d of (7) is used for MTPA control and (9) for FW control. The simulation results showing the behavior of the IPMSM drive under operation in constant torque and field weakening (constant power) regions are illustrated in Fig. 5. The speed command is set at 157 rad/sec and a step change is done at t = 0.4 to a speed 250 rad/sec. T_L is set at 3 N.m. Parameters of the proposed and traditional controllers are selected to give the best performance. As shown, the two controllers during constant torque region provide a similar performance. This is to guarantee a fair comparison. However, if a speed command is changed, the traditional controller gives a degrading performance. The main reason is that it is designed based on certain conditions and prior knowledge of the system parameters. If this information is changed, its performance deteriorates.

The simulation results showing the performance of the IPMSM drive under operation in FW region at speed 250 rad/sec and load torque 3 N.m are illustrated in Fig. 6. These results are provided to compare the traditional PI controller and the proposed PI controller with LTE. It is obvious that the proposed controller with LTE is superior than the traditional PI controller. It has rapid response, small rise time, small settling time, no-overshoot, and no-undershoot. The simulation results showing the performance of the IPMSM under the operation in the FW (constant power) region are shown in Fig. 7 under load torque change from 1 to 3 N.m. It is evident that the speed dip is 1 rad/sec and the recovery time is 100 *msec*. However, the traditional controller has a speed dip of 12 rad/sec and a recovery time of 100 *msec*.

To justify the efficacy of the LTE and its influence on the performance of the IPMSM, Fig. 8 is provided. This figure demonstrates the simulated i_q responses of the proposed PI controller with LTE in the FW region of the IPMSM drive. Three cases are presented during the starting operation in CTR, the step speed change in CPR, and load torque change during the constant power region. The stator current i_q^*, i_{qT_L}, and $i_{q\Delta\omega}$ are shown. As shown, the LTE compensates i_q^* during transients. This gives the superiority of the proposed PI controller with LTE during tracking trajectory and load torque disturbances. As clear, combining LTE with PI controller improves the performance of IPMSM. It ensures low rise time, low settling time, no overshoot or undershoot under speed changes. Also, it provides less speed dip and less recovery time under load torque disturbances. The most adventurous features are no extra sensors and no additional cost.

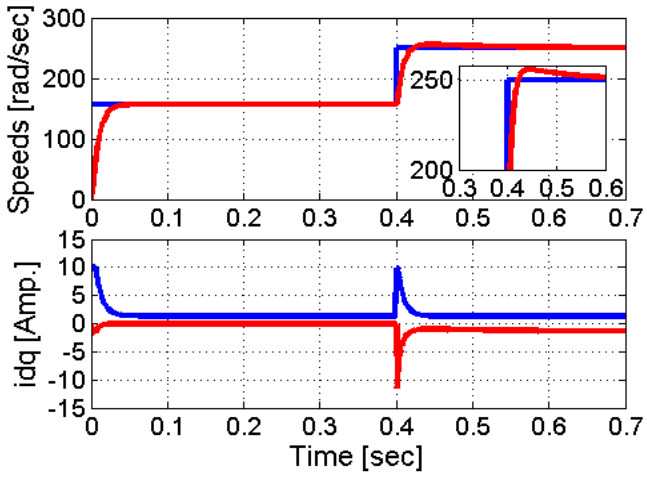

(a) PI controller without LTE

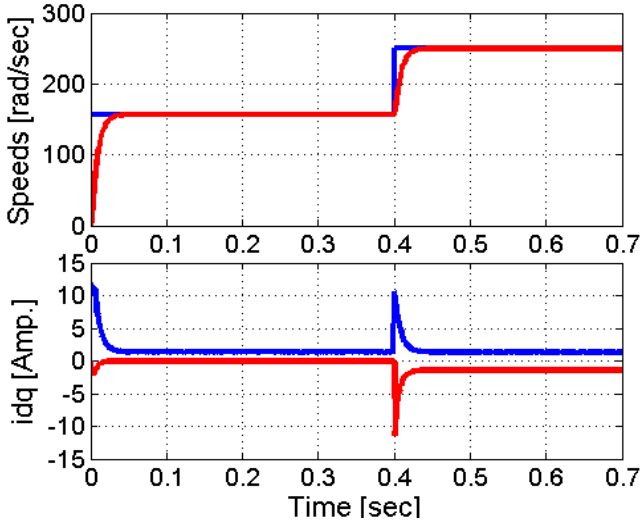

(b) Proposed PI controller with LTE.

Figure 5. Simulation responses of the IPMSM drive in CTR and FW region under a step change of speed command from 0 to 157 to 250 rad/sec

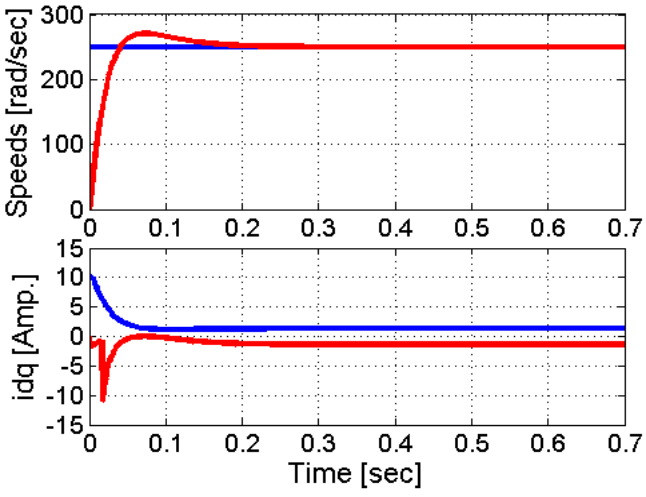

(a) PI controller without LTE

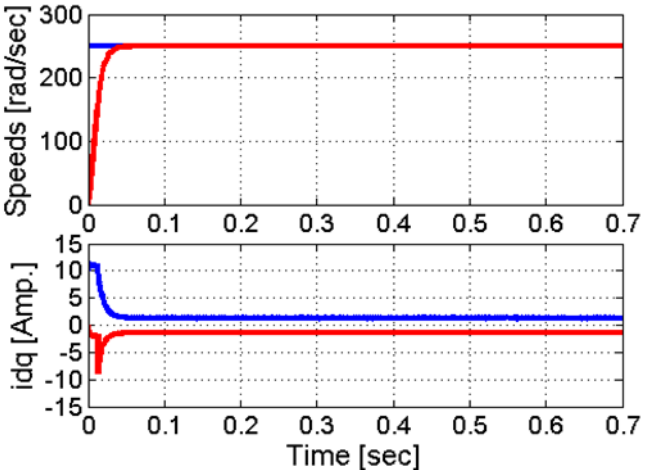

(b) Proposed PI controller with LTE

Figure 6. Simulation responses of the IPMSM drive in FW region under a step change of speed command from 0 to 250 rad/sec

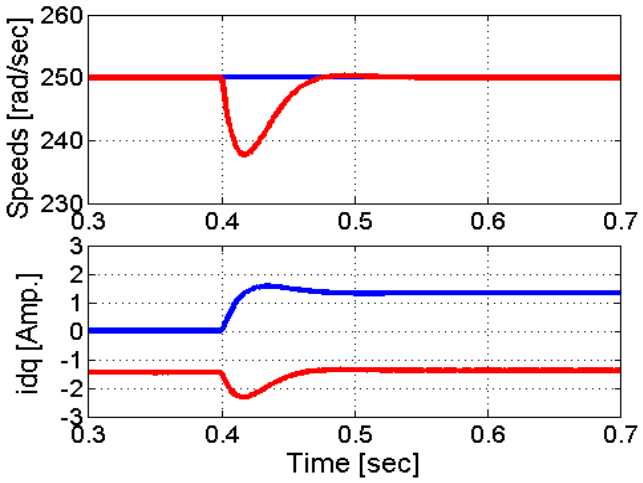

(a) PI controller without LTE

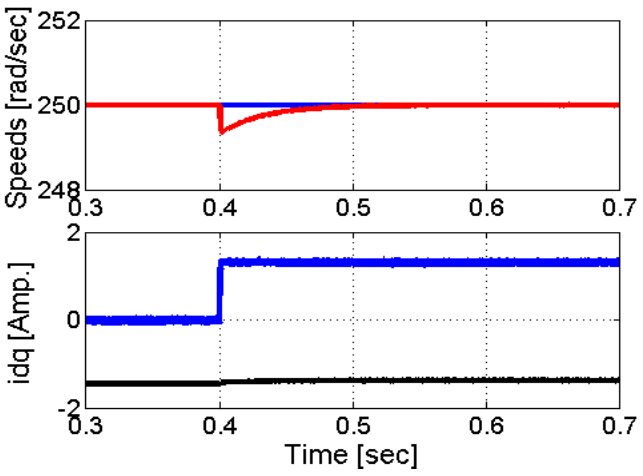

(b) Proposed PI controller with LTE

Figure 7. Simulation responses of the IPMSM drive in FW region under a step load torque variation from 1 to 3 N.m at speed of 250 rad/sec

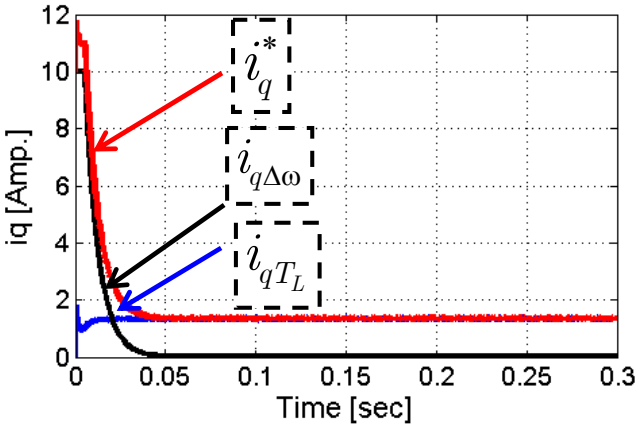

(a)

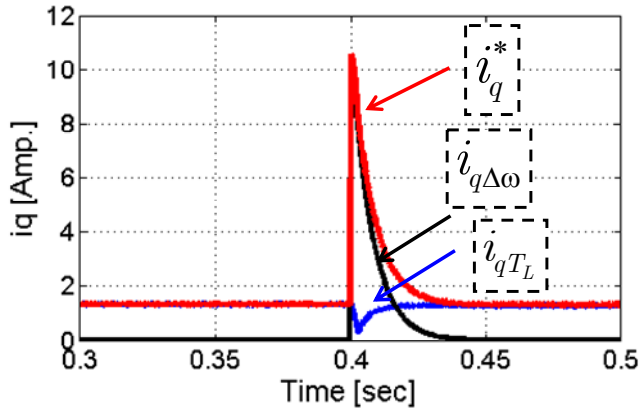

(b)

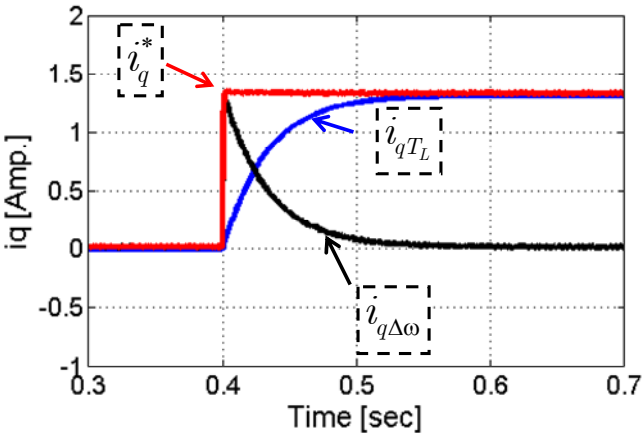

(c)

Figure 8. Simulated stator current responses (iq) showing the behavior of the proposed PI controller with LTE in FW region of the IPMSM drive under speed tracking and load torque. (a) Starting performance. (b) Step speed change. (c) Step load change

VI. IPMSM Drive Setup and Experimental Tests

A. Laboratory Drive Setup

The efficiency of the proposed approach of the PI speed controller with a feed-forward LTE can be proved using the laboratory tests. The laboratory prototype of the IPMSM drive is executed as demonstrated in Fig. 9. The IPMSM drive system is composed from IPMSM, DC generator, voltage source inverter, interface circuits, incremental encoder, current transducers, a DSP-DS1102 control platform, and MATLAB/Simulink program. The IPMSM under control is a 1 HP laboratory machine. DC generator is employed for load applications. The inverter supplies the IPMSM by Pulse Width Modulated (PWM) technique. It

consists of six IGBT's. An interface circuit is utilized to isolate the power circuit from the DSP board. Also, it amplifies the output pulses from the DSP to be suitable for gate excitation. The control platform is based on a dSPACE-DS1102. Two current transducers are used to measure the stator phase currents. The measured currents are sent to the DSP board via A/D acquisition ports. The third current is computed using the two measured ones. An encoder is attached to the rotor shaft to measure the speed. It is 2048 pulses per revolution. The reference speed is compared with the actual one. The speed error is the input to the speed controller either the traditional PI controller or the proposed controller with LTE. The output of the speed controller is i_q. The current i_d is calculated using the speed and i_q. These currents in dq-axis are transformed to the reference stator currents. The measured stator currents are compared with the reference currents based on hysteresis current controller. It can be employed to manage the current within the desired band and to obtain the gate pulses. They are six pulses transmitted from the DSP to switches gate using the output ports and the interface circuit. The procedure of executing the whole drive can be stated by Fig. 10.

B. Experimental Tests

Numerous tests are executed to appraise the behavior of the traditional and the proposed controller with LTE. The MTPA control of IPMSM drives with considering i_d is provided for CTR and CPR using (7) and (9), respectively. Fig. 11 illustrates the experimental tests of the IPMSM drive in CTR and CPR under a step speed from 0 to 157, then from 157 to 250 rad/sec, respectively. Fig. 12 illustrates the experimental tests of the IPMSM in FW region under a step speed command from 0 to 250 rad/sec. It is evident that the speed response using the proposed controller with LTE reaches the steady state smoothly without overshoot. It takes a less settling time to reach the command speed. But, the conventional controller has an overshoot and a high settling time. Experimental speed responses of the IPMSM drive in FW region under a step change of load torque from 1 to 3 N.m at speed of 250 rad/sec are shown in Fig. 13. Three controllers are presented. The traditional PI controller, the proposed PI controller with i_d = 0 and LTE, and the proposed PI controller with $i_d \neq 0$ and LTE. As seen, the traditional PI controller has a dip speed of 20 rad/sec and takes a large recovery time of 450 msec to attain the steady state speed. Nevertheless, the proposed PI controller with i_d = 0 and with LTE gives a better performance than the traditional PI controller. It takes a less recovery time of 300 msec to reach the steady state speed. Alternatively, the proposed PI controller with $i_d \neq 0$ and with LTE provides a significant performance compared to the other two controller types. It has a small speed drop of 3 rad/sec and a small recovery time of 100 msec.

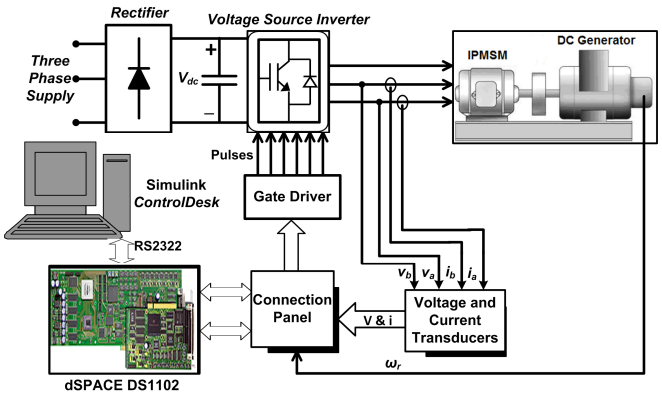

Figure 9. Schematic diagram of the field oriented control of the IPMSM drive

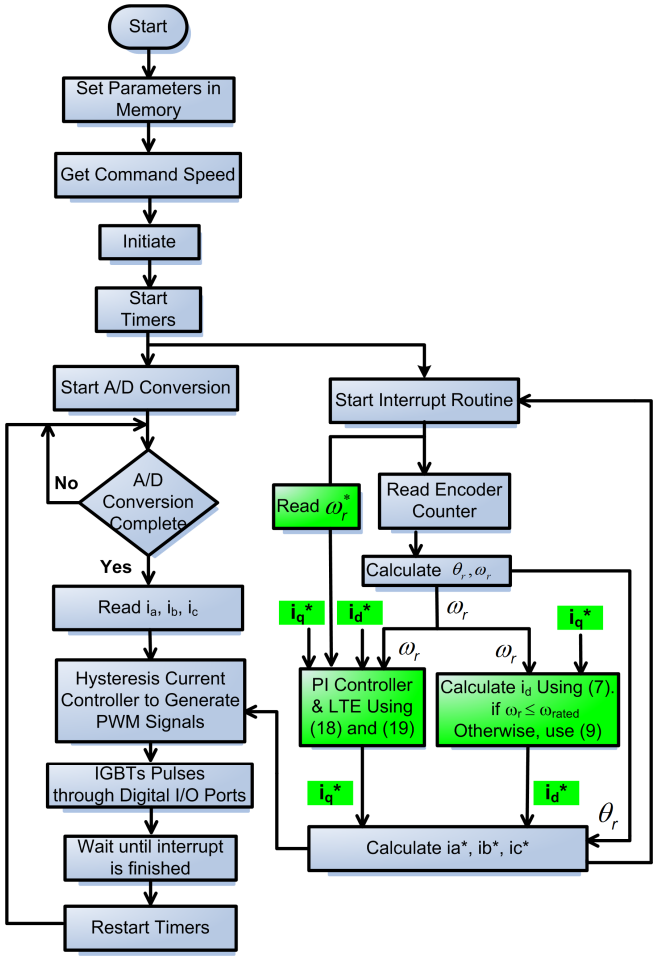

Figure. 10 Flowchart for the software program for execution procedure of the IPMSM drive

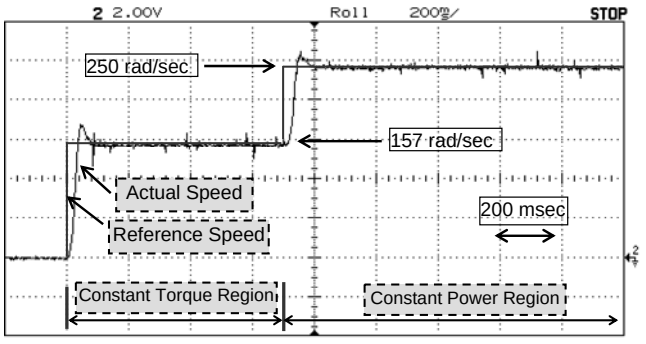

(a) Traditional PI controller

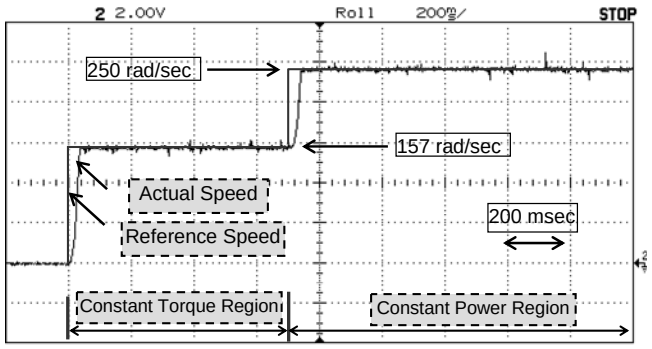

(b) Proposed PI controller with LTE.

Figure 11. Experimental tests of the IPMSM in the CTR and FW under a step speed from 0 to 157 to 250 rad/sec

A fair assessment of the performance of the two controllers is emphasized in Table I. The assessment incorporates the differences between the proposed controller with LTE and the traditional controller in the simulation and experimental tests. The speed response of both the controllers under step speed change and load changes is considered. It is obvious that both the controllers are competitive in some cases. However, the proposed controller proves a superior performance than the traditional controller in most of the cases.

The different tests confirm that the proposed controller using LTE with $i_d \neq 0$ provides excellent speed responses to generate the equivalent quantity of torque. It modifies the speed tracking capability during step speed changes and load torque disturbances without extra sensors and without input-output change.

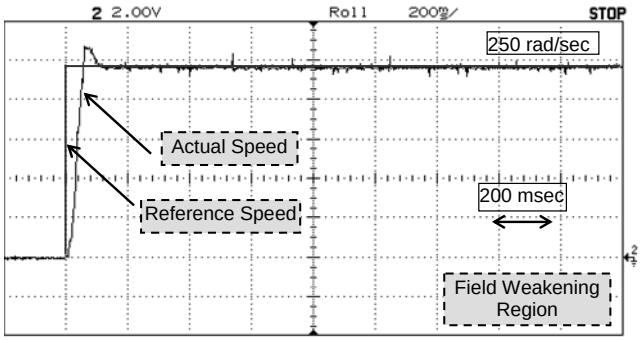

(a) Traditional PI controller

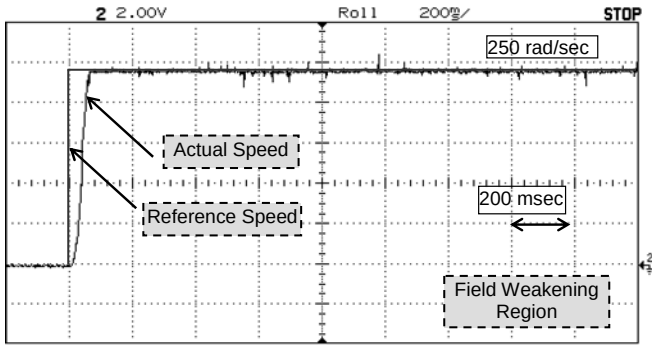

(b) Proposed PI controller with LTE

Figure 12. Experimental tests of the IPMSM in FW under a step speed command from 0 to 250 rad/sec

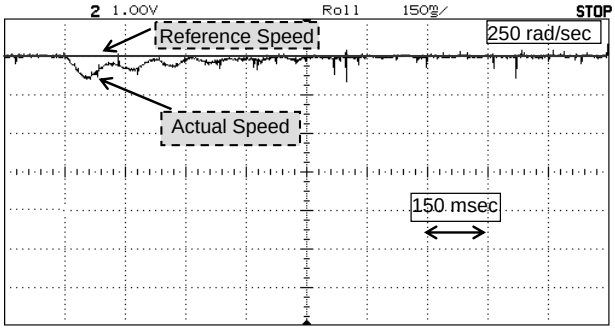

(a) Traditional PI controller with $i_d = 0$

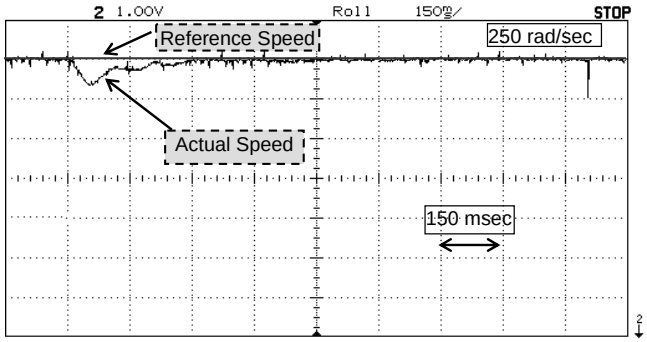

(b) Proposed PI controller without LTE

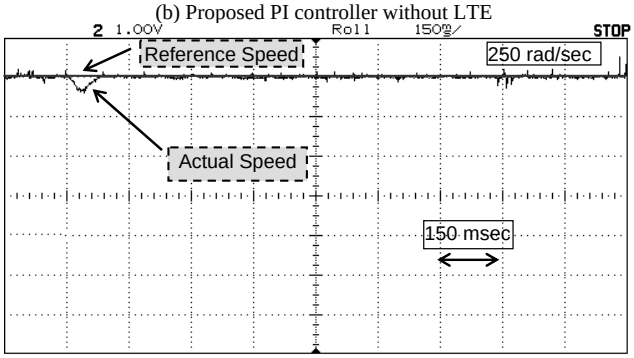

(c) Proposed PI controller with LTE

Figure 13. Experimental tests for IPMSM in FW under a load impact from 1 to 3 N.m at speed of 250 rad/sec

TABLE I. BEHAVIOR CRITERIA OF THE PROPOSED CONTROLLER WITH LTE AND TRADITIONAL ONE.

IM Response		**Simulation Results**		**Experimental Results**	
		Pro.	**Trad.**	**Pro.**	**Trad.**
Speed Response **157 rad/sec**	Rise Time	25 msec	25 msec	40 msec	40 msec
	Overshoot	0 %	%	0 %	%
	Settling Time	30 msec	30 msec	50 msec	100 msec
Speed Response **250 rad/sec**	Rise Time	40 msec	40 msec	70 msec	70 msec
	Overshoot	0 %	7 %	0 %	10 %
	Settling Time	60 msec	140 msec	70 msec	150 msec
Torque Change at **250 rad/sec**	Speed dip	0.4%	4.8 %	1.5 %	8 %
	Recovery time	120 msec	120 msec	100 msec	450 msec

VII. Conclusion

In this paper, an improved PI speed controller of IPMSM drive with a novel LTE has been designed. The MTPA and FW approaches using i_d has been considered. The LTE compensates the speed controller by a feed-forward value. Then, the speed control is decoupled from the load torque. The different results verify the efficiency of the proposed controller with LTE in comparison to the traditional PI speed controller. The two controllers during constant torque region provide a similar performance. This is to guarantee a fair comparison. However, if the speed value changes, the traditional controller gives a degrading performance. The main reason is that it is designed based on certain conditions and prior knowledge of the system parameters. If this information is changed, its performance deteriorates. The proposed LTE-based speed controller with $i_d \neq 0$ provides a precise speed control capability under reference tracking and load changes without extra sensors or changing the input-output hardware of the system. Therefore, it can be suitable for high-performance and low cost industrial applications during a wide speed range without increasing the inverter and motor ratings at FW operation.

Appendix

Table II. Parameters of IPMSM

Rated power (HP)	1	R_s	10.5 Ohm
Phase voltage (Volt)	220	L_d	159 mH
Phase current (Amp.)	1.6	L_q	245 mH
Rated Speed (rpm)	1500	λ_m	0.756 V.S/Rad
Number of poles	4	J	0.003 Kg.m^2
		B	0.00008 N.m/rad/s

References

[1] Y. Cheng, A. Bouscayrol, R. Trigui, “Field weakening control ofa PM electric variable transmission for HEV,” J. Elect. Eng. Technol., vol . 8, no. 5, pp. 1096–1106, Sep. 2013. doi:10.5370/JEET.2013.8.5.1096

[2] K. Kamiev, J. Montonen, M. P. Ragavendra, “Design principles of permanent magnet synchronous machines for parallel hybrid or traction applications,” IEEE Trans. Ind. Electron., vol. 60, no. 11, pp. 4881–4890, Nov. 2013. doi:10.1109/TIE.2012.2221117

[3] C. Mademlis, V.G. Agelidis, “A high-performance vector controlled interior PM synchronous motor drive with extended speed range capability,” in Proc. 27th Annu. Conf. IEEE Ind. Electron. Soc., Nov. 29–Dec. 2, 2001, vol. 2, pp. 1475–1482. doi:10.1109/IECON.2001.976004

[4] J. Wai and T.M. Jahns, “A new control technique for achieving wide constant power speed operation with an interior PM alternator machine,” in Conf. Rec. 36th IEEE IAS Annu. Meeting, Sep. 30–Oct. 4, 2001, vol. 2, pp. 807–814. doi:10.1109/IAS.2001.955545

[5] L. Xu, S. Li, “A fast response torque control for interior permanent magnet synchronous motors in extended flux-weakening operation regime,” in Proc. IEEE Int. Electr. Mach. Drives Conf., 2001, pp. 33–36. doi:10.1109/IEMDC.2001.939269

[6] J. Oyama, K. Ogawa, T. Higuchi, E. Rashad, M. Mamo, M. Sawamura, “Sensorless vector-control of IPM motors over whole speed range,” in Proc. 4th IEEE Int. Conf. Power Electron. Drive Syst., Oct. 22–25, 2001, vol. 2, pp. 448–451. doi:10.1109/PEDS.2001.975357

[7] B. Stumberger, G. Stumberger, D. Dolinar, A. Hamler, M. Trlep, “Evaluation of saturation and cross-magnetization effects in interior permanent-magnet synchronous motor,” IEEE Trans. Ind. Appl., vol. 39, no. 5, pp. 1264–1271, Sep./Oct. 2003. doi:10.1109/TIA.2003.816538

[8] G. H. Kang, J. P. Hong, G. T. Kim, “Nonlinear characteristic analysis of interior type permanent magnet synchronous motor,” in Proc. Int. Conf. IEMD, May 9–12, 1999, pp. 69–71. doi:10.1109/IEMDC.1999.769030

[9] C. T. Pan, S. M. Sue, “A linear maximum torque per ampere control for IPMSM drives considering magnetic saturation,” in Proc. 30th Annu. Conf. IEEE Ind. Electron. Soc., Nov. 2–6, 2004, vol. 3, pp. 2712–2717. doi:10.1109/IECON.2004.1432235

[10] M. N. Uddin, T. S. Radwan, M. A. Rahman, “Performance of interior permanent magnet motor drive over wide speed range,” IEEE Trans. Energy Convers., vol. 17, no. 1, pp. 79–84, Mar. 2002. doi:10.1109/60.986441

[11] J. Lemmens, P. Vanassche, J. Driesen, "PMSM Drive Current and Voltage Limiting as a Constraint Optimal Control Problem," IEEE Journal of Emerging and Selected Topics in Power Electronics, vol. 3, no. 2, pp. 326- 338, June 2015. doi:10.1109/JESTPE.2014.2321111

[12] C. B. Butt, M. A. Hoque, M. A. Rahman, “Simplified Fuzzy-Logic-Based MTPA Speed Control of IPMSM Drive,” IEEE Transactions on Industry Applications, vol. 40, no. 6, pp. 1529- 1535, November/December 2004. doi:10.1109/TIA.2004.836312

[13] C.T. Pan, S.M. Sue, “A linear maximum torque per ampere control for IPMSM drives over full-speed range,” IEEE Transactions on Energy Conversion, vol. 20, no. 2, pp.359-366, June 2005. doi:10.1109/TEC.2004.841517

[14] Y. A. Mohamed, T. K. Lee, “Adaptive Self-Tuning MTPA Vector Controller for IPMSM Drive System,” IEEE Transactions on Energy Conversion, vol. 21, no. 3, pp. 636- 644, September 2006. doi:10.1109/TEC.2006.878243

[15] M. N. Uddin, M. A. Rahman, “High-speed control of IPMSM drives using improved fuzzy logic algorithms,” IEEE Transactions on Industrial Electronics, vol. 54, no. 1, pp.190-199, February 2007. doi:10.1109/TIE.2006.888781

[16] M. N. Uddin, M. M. Chy, “Online Parameter-Estimation-Based Speed Control of PM AC Motor Drive in Flux-Weakening Region,” IEEE Transactions on Industry Applications, vol. 44, no. 5, pp.1486- 1494, September/October 2008. doi:10.1109/TIA.2008.926205

[17] M. N. Uddin, R. S. Rebeiro, “Online efficiency optimization of a fuzzy-logic-controller-based IPMSM drive,” IEEE Transactions on Industry Applications, vol. 47, no. 2, pp. 1043- 1050, March/April 2011. doi:10.1109/TIA.2010.2103293

[18] R. Rebeiro, M. Uddin, "Performance analysis of an FLC-based online adaptation of both hysteresis and PI controllers for IPMSM drive," IEEE Trans. on Ind. Appl., vol. 48, no. 1, pp. 12-19, January/February 2012. doi:10.1109/TIA.2011.2175876

[19] W. Huang, Y. Zhang, X. Zhang, G. Sun, “Accurate torque control of interior permanent magnet synchronous machine,” IEEE Transactions on Energy Conversion, vol. 29, no. 1, pp. 29-37, March 2014. doi:10.1109/TEC.2013.2290868

[20] M. N. Uddin, J. Khastoo, "Fuzzy Logic-Based Efficiency Optimization and High Dynamic Performance of IPMSM Drive System in Both Transient and Steady-State Conditions," IEEE Transactions on Industry Applications, vol. 50, no. 6, pp. 4251- 4259, November/December 2014. doi:10.1109/TIA.2014.2317845

[21] G. Schoonhoven, M.N. Uddin, "MTPA- and FW-Based Robust Nonlinear Speed Control of IPMSM Drive Using Lyapunov Stability Criterion," IEEE Transactions on Industry Applications, vol. 52, no. 5, pp. 4365-4374, September/October 2016. doi:10.1109/TIA.2016.2564941

[22] M. A. Khan, M.N. Uddin, M.A. Rahman, "A Novel Wavelet-Neural-Network-Based Robust Controller for IPM Motor Drives," IEEE Transactions on Industry Applications, vol. 49, no. 5, pp. 2341- 2351, September/October 2013. doi:10.1109/TIA.2013.2261971

[23] G. Schoonhoven, M.N. Uddin, "Harmonic Injection-Based Adaptive Control of IPMSM Motor Drive for Reduced Motor Current THD," IEEE Transactions on Industry Applications, vol. 53, no. 1, pp. 483-491, January/February 2017. doi:10.1109/TIA.2016.2603145

[24] K. Chen, Y. Sun, B. Liu, "Interior Permanent Magnet Synchronous Motor Linear Field-Weakening Control," IEEE Transactions on Energy Conversion, vol. 31, no. 1, pp. 159- 164, March 2016. doi:10.1109/TEC.2015.2478917

[25] M. Tursini, F. Parasiliti, and D. Zhang, “Real-time gain tuning of PI controllers for high-performance PMSM drives,” IEEE Trans. Ind. Appl., vol. 38, no. 4, pp. 1018–1026, Jul./Aug. 2002. doi: 10.1109/TIA.2002.800564

[26] L. Harnefors, S. E. Saarakkala, and M. Hinkkanen, "Speed control of electrical drives using classical control methods," IEEE Trans. on Ind. Appl., vol. 49, no. 2, pp. 889-898, March/April 2013. doi:10.1109/TIA.2013.2244194

[27] M. S. Zaky,” A self-tuning PI controller for the speed control of electrical motor drives,” Electric Power Systems Research, Elsevier, vol. 119 pp. 293–303, February 2015. doi:10.1016/j.epsr.2014.10.004

[28] J. W. Jung, V. Q. Leu, T. D. Do, E. K. Kim, H. Choi, "Adaptive PID Speed Control Design for Permanent Magnet Synchronous Motor

Drives," IEEE Transactions on Power Electronics, vol. 30, no. 2, pp. 900- 908, February 2015. doi:10.1109/TPEL.2014.2311462

[29] H.H. Choi, V.Q. Leu, Y.S. Choi, J.W. Jung, "Adaptive speed controller design for a permanent magnet synchronous motor," IET Electr. Power Applications, vol. 5, Iss. 5, pp. 457–464, Appl., 2011. doi:10.1049/iet-epa.2010.0083

[30] J. Ren, Y. Ye, G. Xu, Q. Zhao, M. Zhu, "Uncertainty-and-Disturbance-Estimator-Based Current Control Scheme for PMSM Drives With a Simple Parameter Tuning Algorithm," IEEE Transactions on Power Electronics, vol. 32, no. 7, pp. 5712- 5722, July 2017. doi:10.1109/TPEL.2016.2607228

[31] M. Preindl, E. Schaltz, "Load torque compensator for model predictive direct current control in high power PMSM drive systems," IEEE Int. Symposium on Ind. Electron. (ISIE), 2010, pp. 1347 – 1352. doi:10.1109/ISIE.2010.5637144

[32] M. Kim, D. Song, Y. Lee, T. Won, H. Park, Y. Jung, M. Lee, "A robust control of permanent magnet synchronous motor using load torque estimation," ISIE 2001, Pusan, KOREA, pp. 1157-1162, 2011. doi:10.1109/ISIE.2001.931642

[33] M.S. Zaky, M.A. Hassanien, S.S. Shokralla, "High dynamic performance of IPMSM Drives based on Feedforward Load Torque Compensator," Electric Power Components and Systems, Taylor & Francis Group, vol. 41, issue 3, pp. 235–251, 2013. doi:10.1080/15325008.2012.742940